Carcinogenesis vol.35 no.8 pp.1788–1797, 2014
doi:10.1093/carcin/bgu053
Advance Access publication March 3, 2014

Myeloid Cell COX-2 deletion reduces mammary tumor growth through enhanced cytotoxic T-lymphocyte function

Edward P.Chen, Nune Markosyan, Emma Connolly, John A.Lawson, Xuanwen Li, Gregory R.Grant, Tilo Grosser, Garret A.FitzGerald, and Emer M.Smyth*

Institute for Translational Medicine and Therapeutics and Department of Pharmacology, University of Pennsylvania, Philadelphia, PA 19104, USA

*To whom correspondence should be addressed. Tel: +215 537 2323; Fax: +215 573 9135;
Email: emsmyth@mail.med.upenn.edu

Cyclooxygenase-2 (COX-2) expression is associated with poor prognosis across a range of human cancers, including breast cancer. The contribution of tumor cell-derived COX-2 to tumorigenesis has been examined in numerous studies; however, the role of stromal-derived COX-2 is ill-defined. Here, we examined how COX-2 in myeloid cells, an immune cell subset that includes macrophages, influences mammary tumor progression. In mice engineered to selectively lack myeloid cell COX-2 [myeloid-COX-2 knockout (KO) mice], spontaneous neu oncogene-induced tumor onset was delayed, tumor burden reduced, and tumor growth slowed compared with wild-type (WT). Similarly, growth of neu-transformed mammary tumor cells as orthotopic tumors in immune competent syngeneic myeloid-COX-2 KO host mice was reduced compared with WT. By flow cytometric analysis, orthotopic myeloid-COX-2 KO tumors had lower tumor-associated macrophage (TAM) infiltration consistent with impaired colony stimulating factor-1-dependent chemotaxis by COX-2 deficient macrophages *in vitro*. Further, in both spontaneous and orthotopic tumors, COX-2-deficient TAM displayed lower immunosuppressive M2 markers and this was coincident with less suppression of $CD8^+$ cytotoxic T lymphocytes (CTLs) in myeloid-COX-2 KO tumors. These studies suggest that reduced tumor growth in myeloid-COX-2 KO mice resulted from disruption of M2-like TAM function, thereby enhancing T-cell survival and immune surveillance. Antibody-mediated depletion of $CD8^+$, but not $CD4^+$ cells, restored tumor growth in myeloid-COX-2 KO to WT levels, indicating that $CD8^+$ CTLs are dominant antitumor effectors in myeloid-COX-2 KO mice. Our studies suggest that inhibition of myeloid cell COX-2 can potentiate CTL-mediated tumor cytotoxicity and may provide a novel therapeutic approach in breast cancer therapy.

Introduction

Cyclooxygenase (COX) converts arachidonic acid into the prostaglandins, a family of lipid mediators that have diverse and widespread biological effects (1,2). Expression of the inducible COX isoform, COX-2, is linked with poor prognosis in breast cancer (2) and its pharmacological inhibition reduces risk across a range of human cancers, including breast (3). In mice, global genetic (4) or pharmacological (5) inhibition of COX-2 suppressed mammary tumorigenesis.

Tumors are comprised of malignant tumor cells and the surrounding microenvironment containing resident and infiltrating non-malignant cells, which release cytokines and growth factors that may impact tumor cell growth. Infiltrating immune cells in the tumor microenvironment display a range of phenotypes and functions. Thus, depending on their differentiation by soluble mediators and expression of surface costimulatory or coinhibitory molecules, tumor-associated immune cells can support or restrain tumor growth. Initially, immune cells are thought to infiltrate the tumor in an effort to eliminate transformed tumor cells; however, their so-called 'reeducation' within the tumor microenvironment suppresses antitumor immune function (6). Macrophages, an important component of the immune microenvironment, are often classified by two phenotypic extremes—classically activated M1, which support inflammation, antigen presentation and cytotoxic generation of reactive oxygen species, or alternatively activated M2, which support angiogenesis, extracellular matrix remodeling and immunosuppression (7). In tumors, cytotoxic T lymphocytes (CTLs), a primary effector cell in tumor elimination, are suppressed through the actions of M2-like tumor-associated macrophages (TAMs) (8) including depletion of extracellular arginine, which is used by CTLs to generate cytotoxic reactive oxygen species (9), and expression of T-cell coinhibitory molecules (10). Additionally, TAMs, recruited by tumor cell-released colony stimulating factor (CSF)-1, produce epidermal growth factor, which, in turn, enhances tumor cell proliferation and survival, thereby forming a critical paracrine loop in which TAM and tumor cells support each other's growth and migration (11). In concordance with these actions, TAM density correlates with poor prognosis in human breast cancer (10,12) and genetic or pharmacological depletion of macrophages in mice delayed mammary tumor progression (13).

COX-2 is integral to macrophage phenotype and function. Inhibition of COX-2 in cultured murine bone marrow cells enhanced differentiation to an antigen-presenting phenotype (14) and suppressed human monocyte to M2 macrophage differentiation (15). The role of COX-2 and its products in determining the phenotype of *in vitro* cultured macrophages or macrophage-like cell lines has been well studied (16,17) though the *in vivo* paracrine and autocrine contribution of COX-2 to macrophage function remain ill-defined. We reported paracrine influences of tumor cell COX-2 to promote mammary tumorigenesis, in part through modulation of TAM and T-lymphocyte function in tumors (18,19). In this study, we investigate deletion of COX-2 in myeloid cells, a subset of immune cells that includes macrophages, and its effect on mammary tumorigenesis using spontaneous and orthotopic models of neu oncogene-induced disease. Deletion of COX-2 in myeloid cells led to reduced tumorigenesis and growth with suppressed macrophage infiltration and enhanced T cells in tumors. This was coincident with decreased CSF-1 receptor levels and reduced M2 marker expression in COX-2 deficient macrophages, suggesting that decreased immune-suppressive M2-like TAMs may contribute to an enhanced effector T cell response. Depletion of $CD8^+$ CTLs restored tumor progression, suggesting that macrophage COX-2 is an important component of suppressed CTL function in mammary tumors and that targeted inhibition of myeloid cell COX-2 may be a useful strategy to limit immune suppression in breast cancer.

Abbreviations: BMDM, bone marrow-derived macrophage; COX, cyclooxygenase; CSF, colony stimulating factor; CTL, cytotoxic T lymphocyte; CV, cardiovascular; DMEM, Dulbecco's modified Eagle's medium; FBS, fetal bovine serum; IL, interleukin; KO, knockout; MDSC, myeloid-derived suppressor cells; MRM, multiple reaction monitoring; mRNA, messenger RNA; Q-PCR, quantitative-PCR; TAM, tumor-associated macrophage; TAN, tumor-associated neutrophils; WT, wild-type.

Materials and methods

Mice

Mouse experiments were conducted in accordance with National Institutes of Health regulations and were approved by the *Institutional Animal Care and Use Committee* of the University of Pennsylvania.

$COX\text{-}2^{flox/flox}$ mice, in which introns 5 and 8 of the COX-2 gene are flanked by loxP sites ('flox'), have been described previously (20). $COX\text{-}2^{flox/flox}$ mice were fully backcrossed onto the FVB/N background (>9 generations) and are denoted as wild-type (WT) mice. $COX\text{-}2^{flox/flox}$ mice were crossed with mice expressing Cre recombinase under the control of the LysM promoter, which directs expression of Cre to cells of myeloid lineage (Cre^{LysM}) (21).

In the resultant COX-$2^{flox/flox}Cre^{LysM}$ mice, COX-2 is knocked out in subsets of myeloid-derived cells, with the primary effect in macrophages and monocytes (22) and are denoted myeloid-COX-2 knockout (KO). WT and myeloid-COX-2 KO mice were crossed with mice expressing an activated rat *c-neu* oncogene (Val^{664}-Glu) under the control of the mouse mammary tumor virus promoter (neu^{mmtv}) to direct expression to mammary epithelial cells (23) (Jackson Laboratory, Bay Harbor, MN) and are denoted WT^{neu} or myeloid-COX-2 KO^{neu}, as appropriate. For all experiments, Cre^{LysM} and neu^{mmtv} were heterozygous and genotypes were verified by PCR (18,22).

Cell lines and culture

NAF and SMF, two cell lines derived from mammary carcinomas harvested from neu^{mmtv} transgenic mice (24), were kindly provided by Dr Lewis Chodosh (University of Pennsylvania). SMF cells were cultured in high-glucose Dulbecco's modified Eagle's medium (DMEM) (Invitrogen) containing 10% calf serum, 0.5% L-glutamine, 1% Pen/Strep and 4 µg/ml insulin ('SMF medium'). NAF cells were maintained in high-glucose DMEM with 10% fetal bovine serum (FBS), 0.5% L-glutamine and 1% Pen/Strep ('10% FBS/DMEM'). To make conditioned medium, SMF (6×10^7 cells in 20 ml SMF medium) were grown for 24 h, washed twice and then incubated in serum-free SMF medium for 24 h and conditioned medium filtered and aliquoted for use in migration experiments (see below).

Luciferase-pcDNA3 (Addgene) plasmid was inserted into pLKO.1-puro lentiviral plasmid vector (Sigma–Aldrich) and packaged into MISSION TRC Lentiviral Particles (Sigma). NAF cells were transduced using MISSION TRC Lentiviral Particles, according to manufacturer's instructions. See Supplementary Materials and methods, available at *Carcinogenesis* Online, for additional details.

L929 cells (American-Type Culture Collection) were maintained in 10% FBS/DMEM as a biological source of CSF-1 for bone marrow-derived macrophage (BMDM) culture (25). L929 cells cultured to 100% confluency in a T75 flask were split 1:5 and cell supernatants collected and stored after a further 4 days of culture.

BMDM isolation, culture and treatments

BMDM were isolated and cultured as described (25,26). Cultured BMDM were serum-starved for 24 h before stimulation with 5 µg/ml lipopolysaccharide (Sigma–Aldrich), M2 polarization cocktail (20 ng/ml interleukin (IL)-4 and 10 ng/ml IL-13, Peprotech) or water as control. After 6 h or 18 h for M2-polarized BMDM, at 37°C, supernatants were collected for eicosanoid measurement by mass spectrometry (described below) and cells were lysed for messenger RNA (mRNA) extraction (RNeasy Mini Kit, Qiagen) for gene expression analysis by quantitative-PCR (Q-PCR); described below), or for protein extraction (radio-immunopreciptiation assay buffer with protease inhibitor; Complete Cocktail Tablet; Roche) for COX-1 and COX-2 protein quantification by liquid chromatography/mass spectrometry in multiple reaction monitoring (MRM) mode (described below). BMDM migration was assessed through a modified Boyden Chamber assay. See Supplementary Materials and methods, available at *Carcinogenesis* Online, for additional details.

Animal experiments

Myeloid-COX-2 KO^{neu} and WT^{neu} mice spontaneously develop tumors after 12 weeks, with 100% of mice tumor bearing by 32 weeks (23). For orthotopic injection of tumor cells, SMF or NAF^{Luc} tumor cells were treated with 0.25% Trypsin (Invitrogen) for 10 min. SMF or NAF^{Luc} cells were resuspended at 1×10^7 cells/ml and injected into the left and right #4 mammary glands of myeloid-COX-2 KO and WT mice between 8 and 14 weeks of age (100 µl/gland; 1×10^6 cells).

For T-cell depletion experiments, mice were intraperitoneally injected with 200 µg isotype control, anti-CD4 or anti-CD8 antibodies (BioXCell) 4 days prior to orthotopic injection of SMF cells. Mice in the CD8 depletion group received a second 200 µg dose of anti-CD8 antibody 2 days prior to tumor cell injection. After tumor cell injection, mice continued to receive isotype control or anti-CD4 antibody treatment once weekly, or anti-CD8 antibody twice weekly, until the study's conclusion. Depletion of CD4 or CD8 T cells was confirmed by flow cytometry of erythrocyte-lysed whole blood (ACK Lysing Buffer, Invitrogen).

Mice with transgenic neu^{mmtv} expression, or orthotopic injection of tumor cells, were palpated twice weekly and considered tumor bearing if a palpable mass persisted for at least 1 week. Age at tumor onset, as determined by palpation, were used in survival analyses. Palpable masses were measured with calipers, with tumor volume expressed as (length × $width^2$)/2. At necropsy, tumors were counted and resected, then flash frozen in liquid nitrogen for mRNA isolation, stored in Prefer (Anatech) overnight and paraffin embedded, or digested for 2 h at 37°C in complete EpiCult-B medium containing 5% FBS and 10% collagenase/hyalurdoninase (StemCell Technologies). RNA was isolated from flash frozen tissue using RNeasy Mini tubes after TissueLyser bead-based homogenization. Digested tissue was collected and treated with 1:4 Hank's Balanced Salt Solution (Invitrogen)/2% FBS: ammonium chloride solution (StemCell Technologies). After one wash, the pellet was treated with 0.25% trypsin and a dispase/DNase solution, filtered and resuspended in phosphate-buffered saline for flow cytometric analysis.

Mice with orthotopic injection of NAF^{Luc} cells were injected with 150 mg/kg D-Luciferin (Gold Biotechnology) dissolved in Dulbecco's phosphate-buffered saline and scanned 15 min postinjection in an IVIS Lumina II (Perkin Elmer) for detection of bioluminescence. Mice were scanned every 3 min for 21 min with data from scans with highest sensitivity (peak counts) used for sequence analysis and normalization.

Flow cytometry

Single cell suspensions (BMDM, digested tumors or erythrocyte-lysed whole blood) were stained using typical procedures. Cells were stained for viability using LIVE/DEAD Fixable Aqua (Life Biotech), followed by Fc Blocking (anti-mouse CD16/CD32, BD Pharmagen) before cell surface stain or fixation/permeabilization (Cytofix/Cytoperm, BD Pharmagen) and intracellular stain. Flow cytometry was performed using a 4-laser LSR II (BD Biosciences). Compensation was performed using OneComp eBeads stained with antibodies of the appropriate fluorophore. See Supplementary Materials and methods, available at *Carcinogenesis* Online, for additional details and antibodies.

Quantitative-PCR

RNA isolated from BMDM or whole tumors isolated above were quantified and reverse transcribed into complementary DNA (MultiScribe Reverse Transcriptase, Applied Biosystems) according to manufacturer's instructions. Q-PCR was carried out using inventoried primer/probe gene expression assays with TaqMan Universal PCR Master Mix (Applied Biosystems) for all genes with the exception of CSF-1R, where the QuantiFast Probe Assay with 2 Step RT-PCR Master Mix with ROX dye (Qiagen) was used. Q-PCR products were monitored using the Viia™ 7 Real-Time PCR System (Applied Biosystems) and data was analyzed using the $2^{-\Delta\Delta Ct}$ method of relative quantification (27) using 18S for normalization and mixed M1/M2 polarized macrophage RNA as a calibrator.

Mass spectrometry

Detection of eicosanoids and their associated metabolites was performed using ultrahigh-pressure liquid chromatography/tandem mass spectrometry with negative electrospray ionization and MRM, as described (28). Quantification of CO proteins was performed by stable-isotope dilution liquid chromatography/mass spectrometry in MRM mode (29). See Supplementary Materials and methods, available at *Carcinogenesis* Online, for additional details.

Immunohistochemistry

Immunohistochemistry was performed using standard procedures. See Supplementary Materials and methods, available at *Carcinogenesis* Online, for additional details and antibody lists.

Statistical analysis

All significance testing was performed with non-parametric two-sample Mann—Whitney tests or Log-rank (Mantel-Cox) tests for survival analysis. Paired tests were performed when appropriate. Statistical analyses were performed using Prism (GraphPad Software). See Supplementary Materials and methods, available at *Carcinogenesis* Online, for details on power analysis and handling of multiple testing.

Results

Confirmation of myeloid/macrophage COX-2 deletion in myeloid-COX-2 KO mice

Myeloid-COX-2 KO mice have been previously characterized on the C57/BL6 background. Though Cre^{LysM} is expressed in all cells of myeloid origin (such as neutrophils, immature monocytes and certain dendritic cells), the primary effect of the Cre^{LysM}-mediated COX-$2^{flox/flox}$ deletion was previously characterized as ablation of COX-2-derived prostaglandins in BMDM and thioglycollate-elicited peritoneal macrophages, with minimal effect on isolated neutrophils and dendritic cells (22). We first established that backcrossing to the FVB/N background, and our use of heterozygous Cre-LysM mice, led to a similar pattern of COX-2 deletion through Q-PCR and COX-2 peptide detection. COX-2 mRNA was reduced (>90%) in BMDM treated with lipopolysaccharide (to induce COX-2 expression; Figure 1A *Left*). By liquid chromatography/mass spectrometry in MRM mode, COX-2 peptide levels were reduced by >50% compared with WT

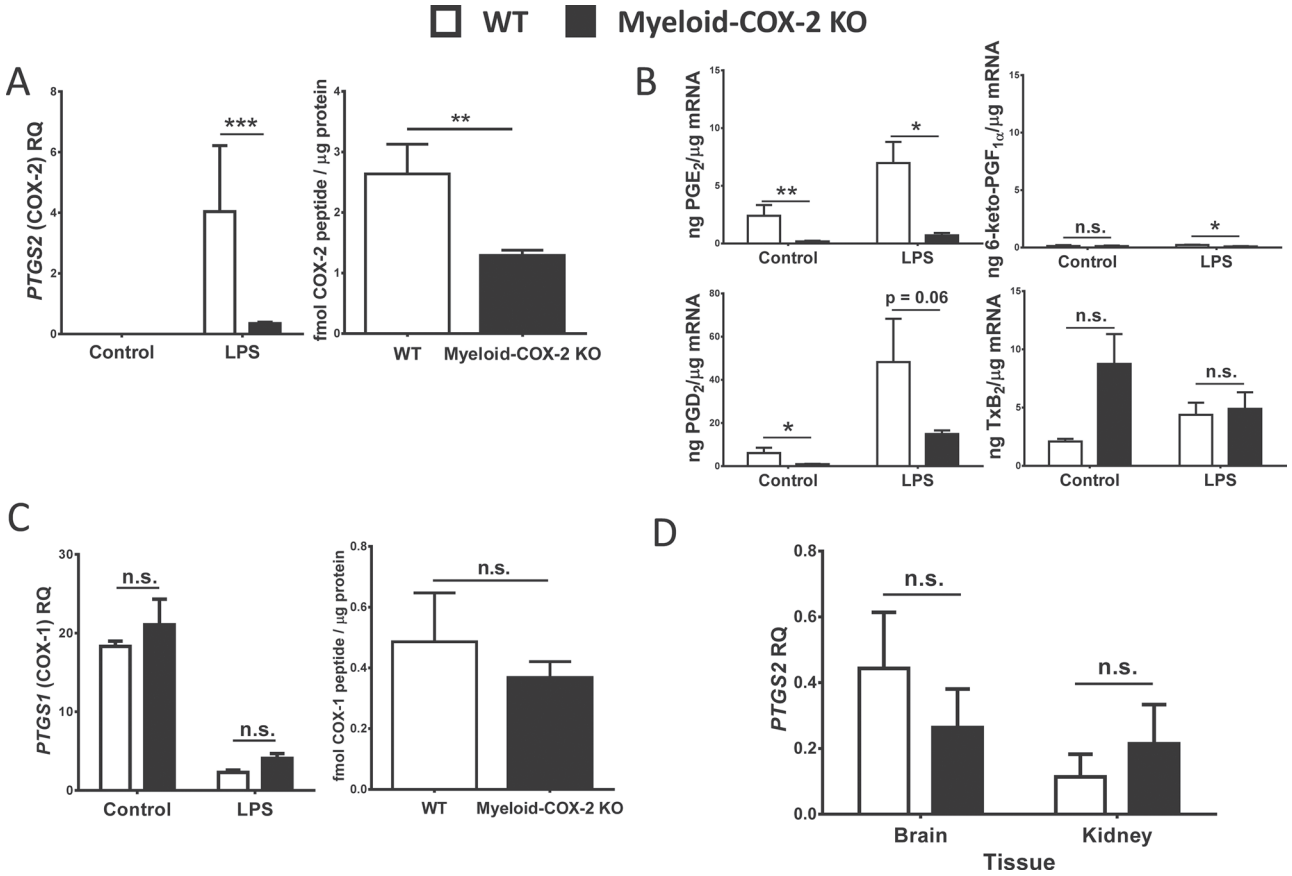

Fig. 1. Selective deletion of COX-2 in myeloid-COX-2 KO mice. BMDM were stimulated with lipopolysaccharide (5 µg/ml, 6 h) to induce COX-2 expression. COX-2 was significantly reduced in myeloid-COX-2 KO compared with WT BMDM by (**A**) Q-PCR for mRNA (*Left*, $n = 6$) and quantification of COX-2 peptide by liquid chromatography/mass spectrometry in MRM mode (*Right*, $n = 5–7$), whereas (**B**) COX-1 expression was unaltered. (**C**) Lipopolysaccharide-induced PGE_2 synthesis in myeloid-COX-2 BMDM was abolished and PGD_2 markedly decreased compared with WT ($n = 3–4$). (**D**) Constitutive (no lipopolysaccharide) COX-2 mRNA levels were not altered in kidney and brain tissue of myeloid-COX-2 KO compared with WT mice ($n = 4$). RQ = relative quantity. Data are mean ± SEM. $*P < 0.05$, $**P < 0.01$, $***P < 0.001$, n.s. = not significant.

(COX-$2^{flox/flox}$LysM-$Cre^{-/-}$; Figure 1A *Right*) and this abolished lipopolysaccharide-induced prostaglandin E2 (PGE_2) generation and markedly reduced PGD_2 generation (Figure 1B). COX-1 protein and mRNA levels were unchanged in myeloid-COX-2 KO BMDM (Figure 1C) and COX-2 mRNA was unchanged in myeloid-COX-2 KO brain or kidney, both of which constitutively express COX-2 (Figure 1D), showing specificity of Cre^{LysM}-directed COX-2 deletion strategy.

Deletion of myeloid cell-COX-2 reduced neu oncogene-induced mammary tumorigenesis

Tumor onset (as determined by detection of a palpable mammary mass persisting for over a week) was significantly delayed, and tumor multiplicity (the number of mammary lesions at necropsy) reduced, in myeloid-COX-2 KO^{neu} mice compared with WT^{neu} mice (Figure 2A and B). Further, tumor growth, as measured by volume of the largest tumor in each animal (Figure 2C) or by the number of weeks for the largest tumor to reach $0.25cm^3$ (Figure 2D), was also significantly reduced in myeloid-COX-2 KO^{neu} mice. Because of the knock-in strategy used, LysM-$Cre^{+/+}$ mice are null for endogenous LysM (21), raising the possibility of confounding effects of lysozyme M knockout. To minimize such confounders, we maintained myeloid-COX-2 KO mice with heterozygous LysM-Cre expression (i.e. COX-$2^{flox/flox}$/LysM-$Cre^{+/-}$), thus retaining one native LysM allele. We further confirmed that the reduced tumor phenotype was not simply due to deletion of one copy of endogenous LysM in our model. Thus, LysM-$Cre^{+/-neu}$ mice (expressing the native mouse COX-2 gene) did not differ from WT^{neu} in tumor onset, multiplicity or growth and remained significantly more diseased compared with myeloid-COX-2 KO^{neu} (Supplementary Figure S1A–C, available at *Carcinogenesis* Online). In a related model, SMF or luciferase-expressing NAF (NAF^{Luc}), which are mouse mammary tumor cell lines derived from neu oncogene transgenic spontaneous mammary tumors (24), were grown as orthotopic tumors in mammary fad pads of syngeneic immune competent host mice. Similar to the spontaneous model, tumor growth was depressed in host myeloid-COX-2 KO mice receiving either SMFs (Figure 2E) or NAF^{Luc} (Figure 2F), compared with WT hosts, and also was unrelated to the deletion of one LysM allele in myeloid-COX-2 KO host mice (Supplementary Figure S1D, available at *Carcinogenesis* Online).

To explore the biology underlying reduced disease burden in myeloid-COX-2 KO mice, we examined indices of proliferation, apoptosis and angiogenesis. No differences were observed in mRNA for caspase-3 (apoptosis) or Ki67 (proliferation) in tumor tissue from myeloid-COX-2 KO compared with WT mice or by immunohistochemical staining for activated caspase-3 or Ki67, in either the spontaneous (Supplementary Figure S2A–C, available at *Carcinogenesis* Online) or orthotopic (Supplementary Figure S3A–C, available at *Carcinogenesis* Online) model. Further, although mRNA for the angiogenic factor vascular endothelial growth factor A was decreased in spontaneous myeloid-COX-2 KO^{neu} tumors, expression of its receptor, VEGFR2, was increased and no difference in tumor vascularization was evident by anti-Von Willebrand Factor immunostaining of tumor sections for vascular endothelium (Supplementary Figures S2D and E, available at *Carcinogenesis* Online). Similarly, there was no evidence for modified vascularization between orthotopic SMF tumors grown in myeloid-COX-2 KO or WT hosts (Supplementary Figures S3D and E, available at *Carcinogenesis* Online).

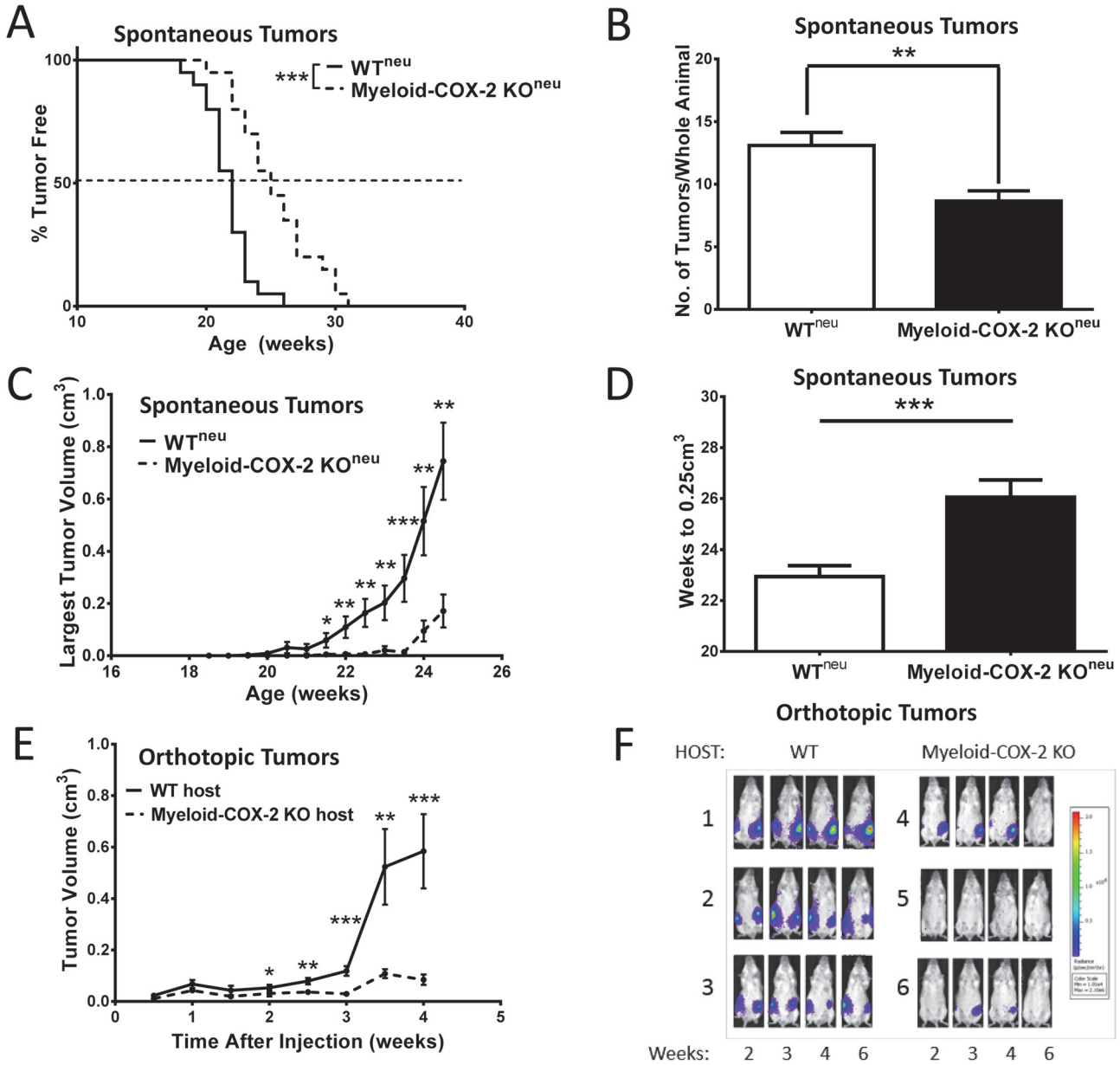

Fig. 2. Deletion of myeloid cell COX-2 reduces tumorigenesis in neu^{mmtv} oncogene-driven spontaneous and orthotopic tumors. (**A**) Tumor onset was delayed ($n = 20$), (**B**) tumor multiplicity reduced ($n = 19$–20) and (**C**) tumors were smaller ($n = 13$–17) in myeloid-COX-2 KO mice transgenic for neu^{mmtv} (myeloid-COX-2 KO^{neu}) compared with WT^{neu} mice. (**D**) Myeloid-COX-2 KO^{neu} tumors were slower to reach a volume of 0.25cm^3 compared with WT^{neu} mice ($n = 18$–19). (**E**) SMF mammary tumor cells grew significantly smaller tumors in myeloid-COX-2 KO recipient mice, compared with WT ($n = 17$–20). (**F**) NAF mammary tumor cells, stably expressing luciferase, were evident earlier in WT, compared with myeloid-COX-2 KO, recipient mice and were sustained over a 6-week period. (B–E) Data are mean ± SEM. $^*P < 0.05$, $^{**}P < 0.01$, $^{***}P < 0.001$ compared with WT.

Deletion of myeloid cell-COX-2 shifts the cellular composition of the immune microenvironment

TAM are a key component in the tumor immune microenvironment contributing to suppression of CTL function, thus enhancing immune escape (30,31). We next explored how deletion of COX-2 in myeloid cells altered the mammary tumor immune microenvironment. Myeloid-derived suppressor cells (MDSC; Gr-1$^+$CD11b$^+$), natural killer cells (CD3$^-$CD8$^+$) and neutrophils (Gr-1$^+$F4/80$^-$), each quantified as a function of total live-gated immune cells by flow cytometric analysis of whole tumors at necropsy (32), appeared unaltered in spontaneous myeloid-COX-2 KO^{neu} compared with WT^{neu} tumors (data not shown). Interestingly, an inverse relationship between TAM (F4/80$^+$CD11b$^+$Gr-1$^-$) and both CD3$^+$CD8$^+$ CTLs (Figure 3A and B) and CD3$^+$CD4$^+$ (encompassing Th1, Th2 and regulatory T cells, T_{REGS}; $R^2 = 0.37$, $P = 0.03$) was evident in spontaneous WT^{neu} but not in myeloid-COX-2 KO^{neu}, tumors. This data suggested impaired T-cell suppression by COX-2-deficient TAM. Concordantly, flow cytometric analysis of SMF orthotopic tumors revealed increased TAM and decreased CD3$^+$ lymphocytes in tumors from myeloid-COX-2 KO hosts compared with WT (Figure 3C and D and Supplementary Figure S4A–C, available at *Carcinogenesis* Online), with no changes in MDSCs, neutrophils or NKs (Supplementary Figure S5, available at *Carcinogenesis* Online). Increased tumor-associated CD3+ T lymphocytes in myeloid-COX-2 KO tumors were also evident by immunohistochemistry (Supplementary Figure S4D, available at *Carcinogenesis* Online). By flow cytometry, both CD4$^+$ and CD8$^+$ lymphocyte subpopulations were elevated in myeloid-COX-2 KO tumors (Figure 3E and F). There was no difference between WT or myeloid-COX-2 KO host tumors in the relative proportion of CD4$^+$ T cells positive for interferon γ (a Th1 cytokine) or IL-4 (a Th2 cytokine;

Figure 3G and H) and a trend toward an increase in $CD3^+FoxP3^+$ cells was non-significant (Figure 3I), indicating that no single subtype of $CD4^+$ T lymphocyte was dominant in myeloid COX-2 KO tumors.

We considered whether increased chemoattraction of T cells could explain increased orthotopic tumor T-cell density in myeloid-COX-2 KO host mice. However, we observed no difference in CXCL9, CXCL10 or CCL5 expression, three major T-cell chemoattractants expressed by macrophages (33), by flow cytometry, Q-PCR or immunostaining of TAM or BMDM (data not shown). Together these data suggest that increased migration of T cells is not responsible for increased T-cell density in myeloid-COX-2 KO tumors.

Chemotactic migration and phenotype is altered in COX-2-deficient macrophages

Thus far, the data indicated that deletion of myeloid cell COX-2 modified the tumor microenvironment in favor of augmented T-lymphocyte function. We next asked how deletion of myeloid cell COX-2 modified TAM biology. The cytokine CSF-1, acting on its receptor CSF-1R, is essential for the proliferation, migration and maturation of macrophages (34) and drives a critical protumor macrophage–tumor cell paracrine loop (11). We investigated whether CSF-1/CSF-1R contributed to reduced orthotopic TAM density in myeloid-COX-2 KO host mice. Compared with WT cells, naive myeloid-COX-2 KO BMDM displayed significantly decreased CSF-1R by Q-PCR for mRNA (Figure 4A) and by flow cytometry for cell surface expression (Figure 4B). Further, although *in vitro* cell growth was comparable (data not shown), dose-dependent migration of myeloid-COX-2 KO BMDM toward recombinant CSF-1 was abolished compared with WT cells (Figure 4D), suggesting that reduced CSF-1-dependent migration may contribute to lower TAM density in orthotopic tumors grown in myeloid-COX-2 KO hosts. Consistent with this notion, suppressed migration of myeloid-COX-2 KO BMDM toward SMF tumor cell-conditioned medium was evident and reproduced in WT BMDM experiments by pretreatment of conditioned medium with a CSF-1 neutralizing antibody (Figure 4E). Thus, impaired migration of myeloid-COX-2 KO BMDM towards conditioned medium appeared due to a reduced response to tumor-derived CSF-1. Interestingly, CSF-1R surface expression was not different between TAM harvested from myeloid-COX-2 KO and WT host mice (Figure 4C). Similarly, when WT and myeloid-COX-2 KO BMDM that were first polarized *in vitro* to the TAM-like M2 phenotype, suppressed CSF-1R expression in WT cells equalized the genotypes (Figure 4A). Thus, macrophage COX-2 appears more relevant to regulation of CSF-1R expression and function in macrophages prior to their 'education' in the tumor microenvironment.

Macrophage phenotype plays an important role in determining T-cell phenotype. M2-like macrophages, which characteristically express high levels of the enzyme arginase-1, promote T-cell anergy through extracellular arginine depletion (9,14) and through upregulation of T-cell coinhibitory molecules (35,36). We examined whether

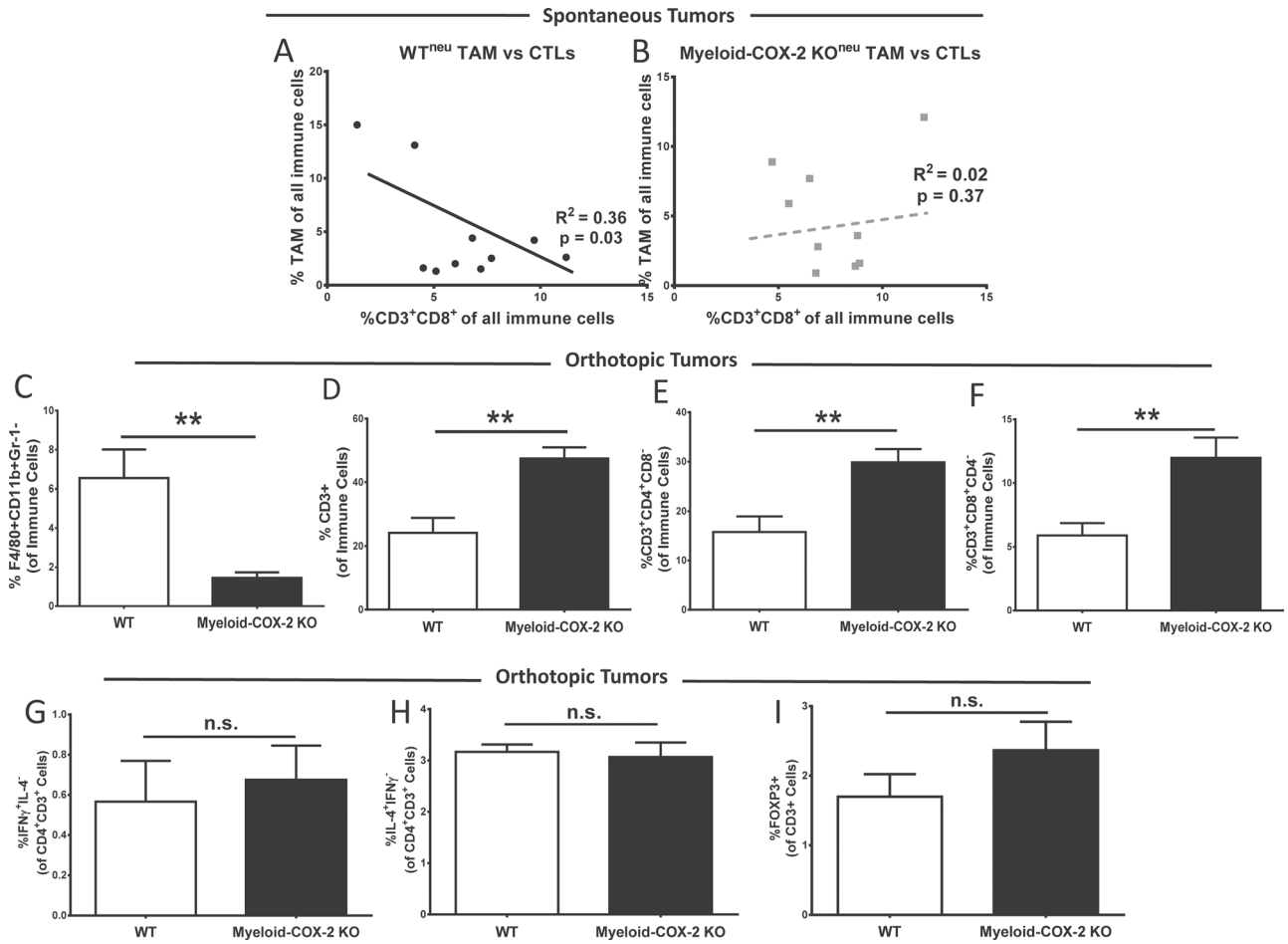

Fig. 3. Myeloid-COX-2 KO tumors display a modified immune microenvironment with less suppression of T lymphocytes. Flow cytometric analysis of enzymatically digested spontaneous tumors indicated that total TAM and $CD3^+CD8^+$ CTLs, as a percentage of tumor immune cells, were inversely correlated in (**A**) spontaneous WT^{neu} tumors ($n = 10$) but not in (**B**) spontaneous myeloid-COX-2 KO^{neu} tumors ($n = 9$). Flow cytometry of digested orthotopic tumors revealed (**C**) reduced TAM density and (**D**) enhanced T-cell density in myeloid-COX-2 KO host tumors compared with WT hosts ($n = 4$–6). The proportion of both (**E**) $CD3^+$ $CD4^+$ T lymphocyte and (**F**) $CD3^+$ $CD8^+$ CTL populations was increased in myeloid-COX-2 KO tumors compared with WT tumors ($n = 7$). No difference was observed between genotypes in the proportion of $CD4^+CD3^+$ T cells positive for (**G**) IL-4, (**H**) interferon γ or (**I**) FOXP3 ($n = 3$–4). Data are mean ± SEM. $^{**}P < 0.01$, n.s. = not significant.

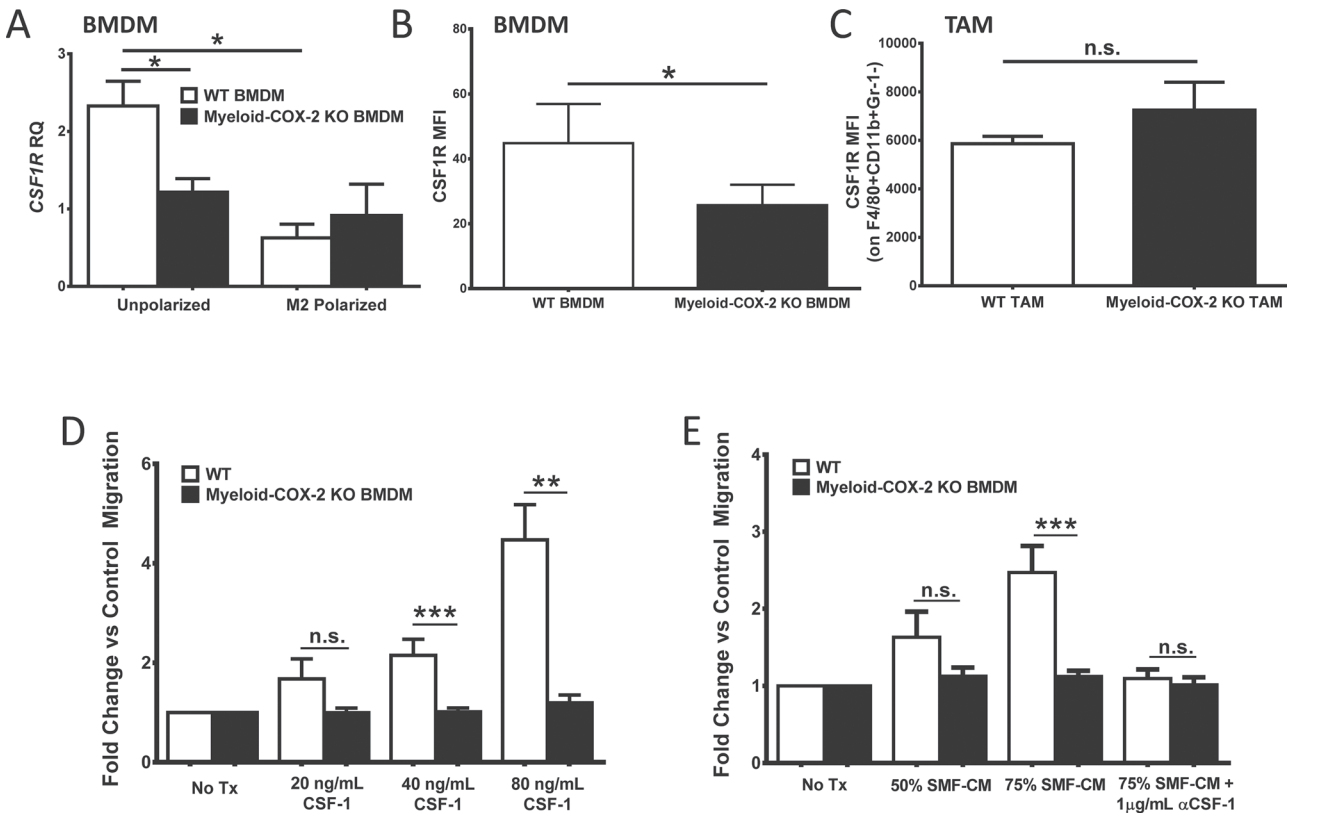

Fig. 4. Deletion of myeloid cell COX-2 reduces macrophage CSF-1R expression and migration. (**A**) CSF-1R expression was lower in naive myeloid-COX-2 KO BMDM compared with WT by Q-PCR for mRNA. M2 polarization (20 ng/ml IL-4 and 10 ng/ml IL-13, 18 h) reduced CSF-1R expression in WT BMDM but did not further modify levels in myeloid-COX-2 KO ($n = 6$). (**B**) By flow cytometry, CSF-1R surface expression was reduced in myeloid-COX-2 KO BMDM compared with WT ($n = 4$) although (**C**) TAM surface CSF-1R expression was not different between genotypes ($n = 3$–4). Migration of myeloid-COX-2 KO BMDM was significantly reduced compared with WT BMDM toward (**D**) CSF-1 or (**E**) conditioned medium from SMF tumors cells (SMF-CM, $n = 5$–10). Addition of CSF-1 neutralizing antibody (αCSF-1) ablated WT BMDM migration toward SMF-CM ($n = 3$). MFI = mean fluorescence intensity; RQ = relative quantity. Data are mean ± SEM. $^*P < 0.05$, $^{**}P < 0.01$, $^{***}P < 0.001$, n.s. = not significant.

TAM phenotype was altered in myeloid-COX-2 KO host tumors. Gene expression analysis of whole tumors indicated reduced expression of M2 marker arginase-1, the M2-associated cytokine IL-10 and the proinflammatory M1 markers iNOS, CD86 and IL-6 in myeloid-COX-2 KO host tumors (Figure 5A), consistent with the lower number of TAMs in myeloid-COX-2 KO tumors. Within the TAM population, flow cytometric analysis indicated that, beyond the lower TAM density in myeloid-COX-2 KO tumors (see Figure 3C), intracellular expression of arginase-1, and another M2 marker CD206, was significantly reduced in TAM from myeloid-COX-2 KO compared with WT hosts (Figure 5B). Further, suppressed arginase-1 and CD206 levels were also evident by flow cytometry of TAM from spontaneous myeloid-COX-2 KO^{neu} tumors compared with WT^{neu} (Figure 5C). These data suggest an autocrine function of macrophage COX-2 in promoting an M2 TAM phenotype. Flow cytometry of TAM for CD86, iNOS and tumor necrosis factor α did not reveal any difference between WT and myeloid-COX-2 KO in either spontaneous (data not shown) or orthotopic models (Figure 5B), suggesting no contribution of macrophage COX-2 to M1 TAM phenotype in this disease model. Taken together, these data suggest reduced immunosuppressive function of COX-2-deficient TAM, consistent with the lower levels of T-cell suppression in myeloid-COX-2 KO tumors from both models.

Depletion of CD8$^+$ T cell restores mammary tumor progression in myeloid-COX-2 KO hosts

As both CD4$^+$ and CD8$^+$ T cells were positively impacted by deletion of myeloid cell COX-2, we sought to determine the contribution of each T-cell subset to reduced mammary tumor growth in myeloid-COX-2 KO mice. We employed antibody-mediated CD4$^+$ and CD8$^+$ T-cell depletion to investigate how each subset individually contributed to orthotopic tumor growth in myeloid-COX-2 KO and WT host mice. Whole blood, after red blood cell lysis, was used to confirm selective depletion of CD4$^+$ or CD8$^+$ T cells (Figure 6A). Depletion of CD4$^+$ T cells did not significantly alter tumor growth in either WT or myeloid-COX-2 KO hosts compared with isotype control-treated mice (Figure 6B). In marked contrast, depletion of CD8$^+$ T cells restored growth of orthotopic mammary tumors in myeloid-COX-2 KO mice close to levels seen in WT host mice (Figure 6C). These data strongly implicate CD8$^+$ CTLs, but not CD4$^+$ T cells, as the T-lymphocyte population responsible for reduced tumor growth in myeloid-COX-2 KO mice. Thus, decreased total and M2-like immunosuppressive TAMs in myeloid-COX-2 KO mice probably reverse suppression of tumoricidal CTLs, reducing tumorigenesis and growth.

Discussion

The marked increase in our understanding of how stromal cells regulate tumor progression has focused attention on therapeutic modulation of the tumor microenvironment (37). Immune surveillance suppresses tumor growth through the cytolytic actions of CTLs and natural killer cells, as well as reactive oxygen species generation by M1 macrophages promoting apoptosis (7). However, reeducation of immune cells by tumors results in immunosuppression encouraging tumor growth. Significant efforts are now being placed on modulating the tumor immune microenvironment to promote immune destruction of tumor cells (36,38), emphasizing the need to define appropriate molecular targets in the tumor microenvironment.

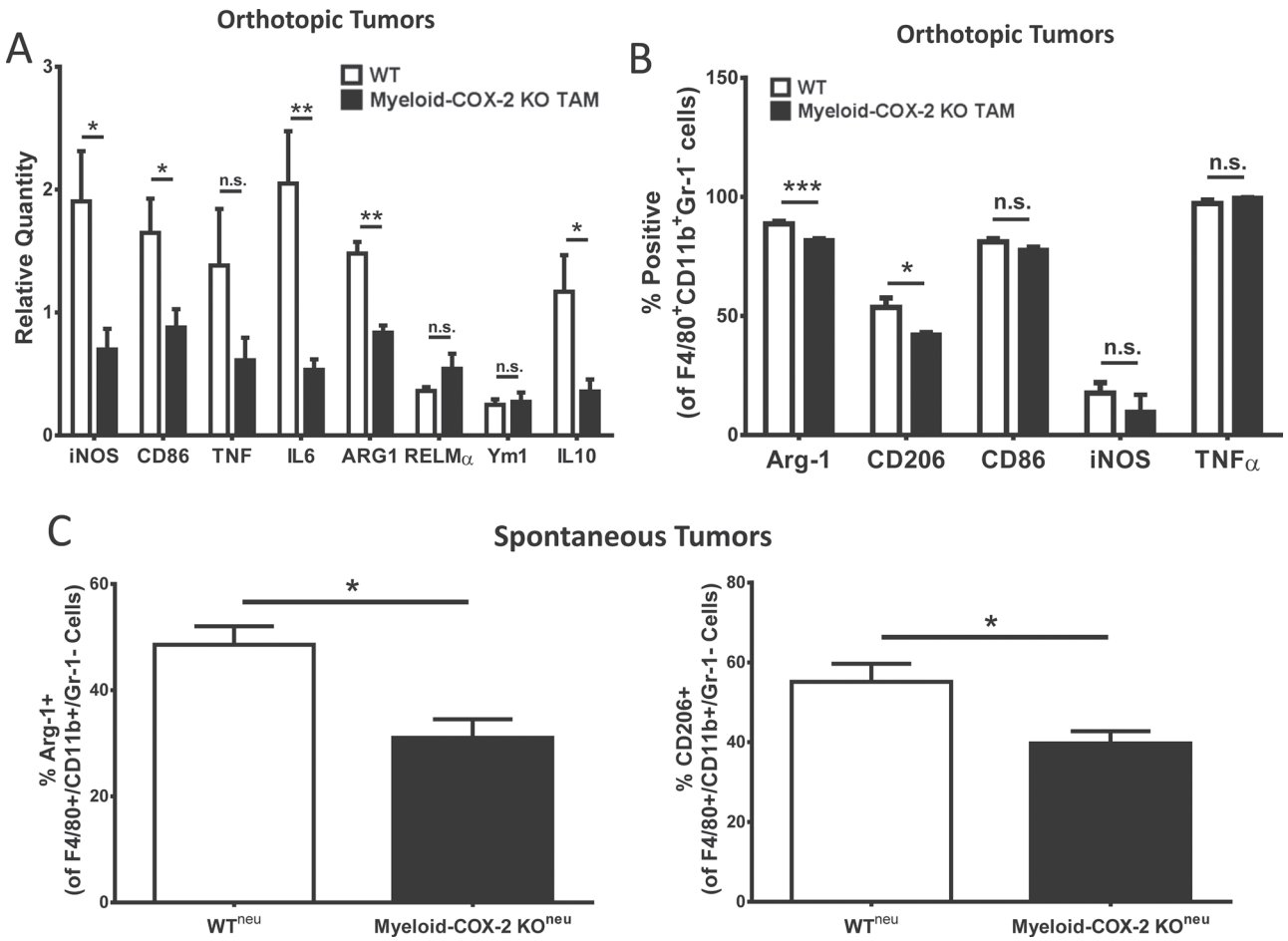

Fig. 5. TAM in myeloid-COX-2 KO mice display an altered macrophage phenotype. (**A**) Q-PCR for mRNA levels of several M1 (iNOS, CD86, IL-6) and M2 (arginase-1 and IL-10) markers were lower in tumor tissue isolated from myeloid-COX-2 KO hosts compared with WT ($n = 4–6$). (**B**) Flow cytometric analysis of live-gated TAMs ($F4/80^+CD11b^+Gr\text{-}1^-$; see Supplementary Figure 4) revealed a lower proportion of M2 (arginase-1 or mannose receptor, CD206, positive) TAMs with no change in M1 (CD86, iNOS or tumor necrosis factor α positive) TAMs in myeloid-COX-2 KO orthotopic tumors compared with WT ($n = 3–6$). (**C**) The proportion of arginase-1 and CD206 positive TAM was also reduced in spontaneous neu-driven tumors ($n = 5–6$). Data are mean ± SEM. $^*P < 0.05$, $^{**}P < 0.01$, $^{***}P < 0.001$, n.s. = not significant.

Despite consensus that interruption of COX-2 function reduces tumorigenesis in animal models of breast cancer (4,5,18,19) and reduces risk in human breast and other cancers (3), an established cardiovascular (CV) hazard associated with selective COX-2 inhibitors (39) severely limits their clinical use. This hazard arises because in addition to the desired inhibition of COX-2 in the tumor, unwanted collateral loss of vascular endothelial COX-2 reduces biosynthesis of prostacyclin, an antithrombotic CV protective agent (39). By avoiding loss of vascular COX-2-derived prostacyclin, specifically targeting COX-2 inhibition to protumor cells may reduce the CV hazard while providing the desired antitumor outcome. Most studies of COX-2 in cancer have focused on global inhibition of COX-2, or on COX-2 in the tumor cells themselves, as a therapeutic target (5,18,19). To the best of our knowledge, ours is the first study to specifically investigate myeloid cell COX-2 deletion in tumorigenesis.

Deletion of myeloid COX-2 substantially reduced mammary tumorigenesis and growth in spontaneous and orthotopic models of neu oncogene-induced breast cancer. Surprisingly, despite this robust phenotype, we observed no difference in markers of apoptosis or proliferation between myeloid-COX-2 KO and WT tumors in tumors from either model. Further, although both COX-2 and TAM have been independently implicated in supporting tumor angiogenesis (4,13,19), vascularization of WT and myeloid-COX-2 KO tumors was not markedly altered. However, we did observe a substantial change in the composition of the tumor microenvironment such that the inverse relationship between TAM and T cells in WT tumors, which reflects the established immunosuppressive functions of TAM (30,40), was offset in myeloid-COX-2 KO mice. This was particularly evident in orthotopic tumors from myeloid-COX-2 KO host mice, where reduced TAM density was mirrored by increased tumor infiltrating T lymphocytes.

Two functional changes in COX-2-deficient macrophages may contribute to this antitumor microenvironmental shift. First, expression of CSF-1R, the receptor for CSF-1 was reduced in COX-2-deficient BMDM. CSF-1, a primary regulator of tissue macrophages and a key component for macrophage recruitment to tumors, is strongly linked with tumor progression and poor outcome in breast cancer (10,41). Further, a critical paracrine loop exists in which tumor cell production of CSF-1 recruits macrophages and encourages their growth, whereas macrophages in turn produce epidermal growth factor, further promoting tumor cell growth (11). We determined a marked disruption of CSF-1 chemokine function that abolished migration of myeloid-COX-2 KO BMDM toward CSF-1 or mammary tumor cell-conditioned medium. It is likely, therefore, that reduced TAM density in the orthotopic myeloid-COX-2 KO tumors results from their reduced chemotactic movement into tumors. Within the tumor microenvironment, however, CSF-1R expression on WT and myeloid-COX-2 KO TAM normalized, suggesting distinct regulation of macrophage CSF-1R in response to extratumoral and intratumoral influences.

Second, the immunosuppressive phenotype that is characteristic of TAM and central to their protumorigenic functions (30,42) was blunted in COX-2-deficient macrophages. TAMs, which augment

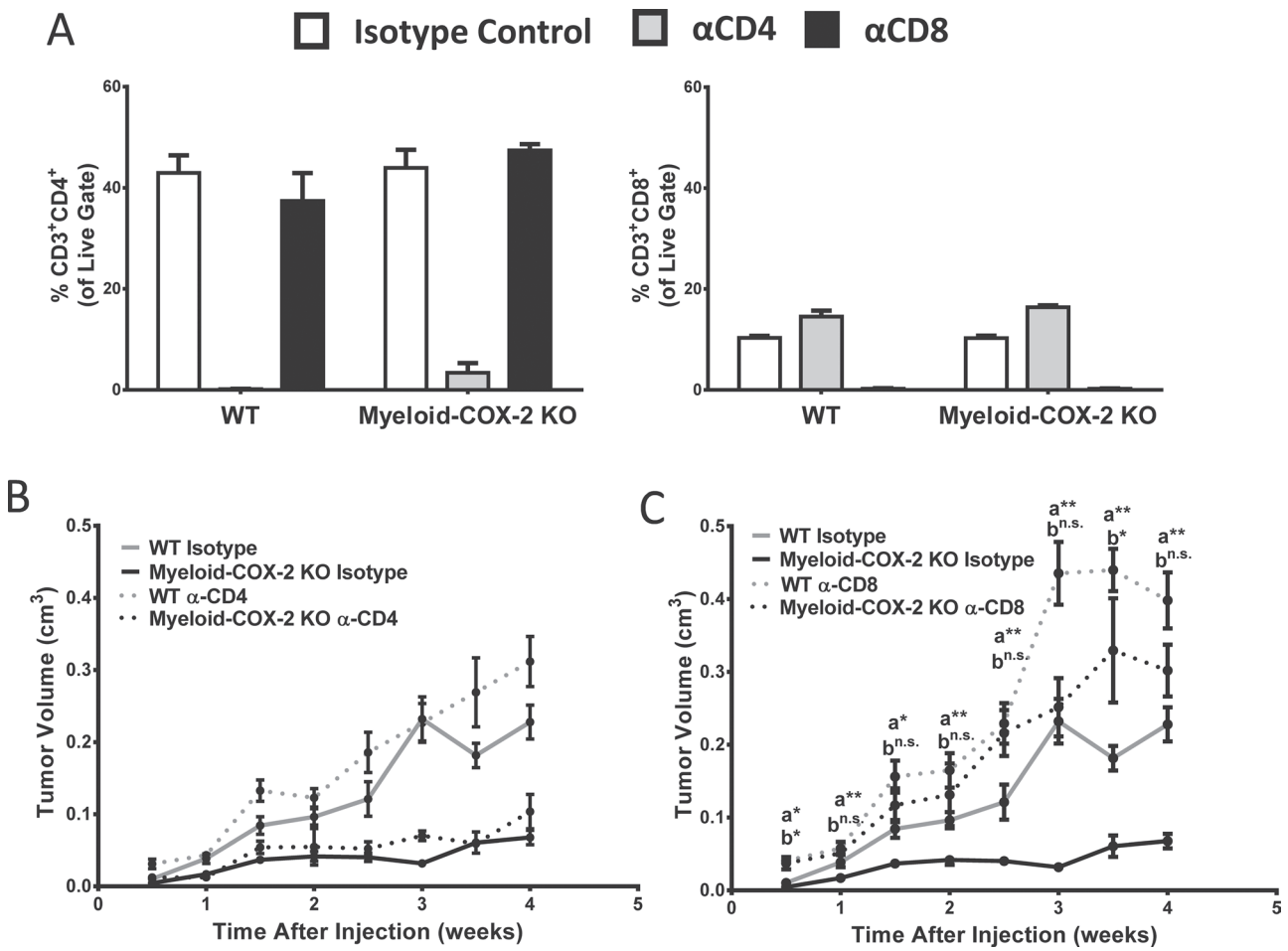

Fig. 6. Antibody depletion of CD8⁺ cells restores orthotopic tumor growth in myeloid-COX-2 KO mice. (**A**) Depletion of CD4⁺ (*right)* or CD8⁺ (*left*) T cells in mice treated with an anti (α)-CD4 or α-CD8 antibody was confirmed by flow cytometry of red blood cell-lysed whole blood ($n = 3$). (**B**) Depletion of CD4⁺ T cells did not significantly alter tumor growth in myeloid-COX-2 KO or WT mice ($n = 6$). (**C**) Depletion of CD8⁺ T cells increased tumor growth in WT mice and restored tumor growth in myeloid-COX-2 KO to WT levels ($n = 6$). Data are mean ± SEM. [a]Comparison between myeloid-COX-2 KO isotype versus myeloid-COX-2 α-CD8; [b]Comparison between WT isotype versus myeloid-COX-2 KO α-CD8, $*P < 0.05$, $**P < 0.01$, n.s. = not significant.

immunosuppression through arginine depletion and expression of coinhibitory molecules leading to T-cell anergy (10), resemble M2 macrophages (14), markers of which were reduced in myeloid-COX-2 KO tumors by mRNA and flow cytometry. The mechanism through which COX-2 deficiency reduced 'M2-ness' of TAM is not clear and may involve both paracrine and autocrine influences of COX-2-derived products. A role for paracrine COX-2 products in promoting tumor-induced M2 polarization, and associated tumorigenesis, has been reported (18,43). In addition, pharmacological inhibition of COX-2 in bone marrow cells enhanced differentiation toward an M1 phenotype (14) and blocked polarization to an M2 phenotype (15), suggesting an autocrine COX-2 influence on macrophage phenotype. Supporting this concept, interference with NFκB signaling, which is established to induce COX-2 expression (44,45), in adoptively transferred BMDM or TAM led to suppressed M2-like phenotype with coincident reduction in tumor growth of an ovarian tumor cell line (46). Likewise, deletion of the NFκB p50 subunit led to an enhanced M1-like TAM phenotype and a reduced growth of a transplanted sarcoma cell line (40). Further, given reports that CSF-1 induces M2 phenotypic marker expression in BMDM (47,48), it may be that the two phenomena we defined in myeloid-COX-2 KO mice, reduced macrophage CSF-1R expression and reduced M2 mammary TAM polarization, are functionally linked.

TAM can suppress T cells through STAT1 signaling and associated induction of arginase-1 (49). Concordantly, in myeloid-COX-2 KO tumors, reduced M2-like TAMs was accompanied by an increase in the proportion of T cells, restoring immune surveillance and reducing tumor growth. Importantly, the internal consistency of reduced TAM immune-suppressive phenotype in both orthotopic and spontaneous models supports the conclusion that myeloid cell COX-2 plays a central role in TAM-mediated support of tumor growth.

Cre^{LysM}-mediated excision of $COX\text{-}2^{flox/flox}$ primarily impacts prostaglandin production by macrophages (22), the major focus of our study. However, multiple cell types of myeloid origin express Cre^{LysM}, including MDSCs and granulocytes, such as neutrophils, and the potential contribution of these cell populations should not be discounted. Of particular importance are MDSCs, which express both arginase-1 and iNOS, may contribute to suppression of T cells resulting in reduced tumor immunosurveillance (16), and tumor-associated neutrophils (TAN), which suppresses activation of CD8⁺ T cells(50). Indeed, PGE_2 enhanced bone marrow cell differentiation in MDSCs (51) and knockout of PGE_2 receptor EP2 reduced MDSC tumor infiltration in a xenograft model of mammary tumorigenesis (51). Though COX-2 in TAN is not well studied, there is evidence in other disease models that COX-2 inhibition may impact migration of neutrophils (52) and that COX-2 expression is correlated with expression of certain neutrophil markers (53). Similar to TAM, protumorigenic and antitumorigenic phenotypes are associated with TAN (50) although a role for COX-2 in TAN differentiation remains unexplored. In our study, although the proportion of MDSCs and neutrophils in the spontaneous or orthotopic models were unaffected by myeloid cell COX-2 deletion, it remains possible that loss of COX-2 in these cells may contribute to reduced tumorigenesis.

As with other immune cells, the specific subtype of the T cell defines its contribution to tumor progression, with Th1 and CTLs performing antitumor functions, whereas Th2 and T_{REGS} supporting tumor growth (10). Since all subpopulations of T cells appeared elevated in myeloid-COX-2 KO tumors, it was unclear to what extent helper or effector T cells contributed to reduced tumor growth. In human breast tumors, high CTL density is associated with increased survival (10), leading us to speculate that reduced tumor growth results from the increase in $CD8^+$ tumor infiltrating CTLs. Indeed, depletion of $CD8^+$ cells in myeloid-COX-2 KO host mice restored orthotopic tumor growth to WT levels, at least through the first 2.5 weeks postinjection, indicating that CTLs are the dominant T-cell subset reducing mammary tumorigenesis. In contrast, there was no impact of $CD4^+$ T-cell depletion in either WT or myeloid-COX-2 KO host mice, probably because equivalent offset of both tumor suppressing Th1 cells and tumor-promoting Th2 cells negates any effect on tumor growth. Interestingly, as tumors continued to grow beyond 2.5 weeks in $CD8^+$-depleted mice, a modest antitumorigenic influence of myeloid cell COX-2 deletion emerged suggesting that, although $CD8^+$ CTLs are a major driver in reduced tumorigenesis in myeloid-COX-2 KO mice, additional mechanisms may contribute to reduced disease. These mechanisms may include reduced M2 effector functions of myeloid-COX-2 KO TAMs, such as the formation of tumor-promoting L-arginine metabolites, or a loss of myeloid cell-derived paracrine COX-2 products, like PGE_2, driving cancer signaling pathways, such as transactivation of epidermal growth factor receptor (54,55) or overexpression of antiapoptotic Bcl-2 (56).

Recently, we reported a similar suppression of mammary tumorigenesis in mice lacking COX-2 specifically in mammary epithelial cells (MEC–COX-2 KO), with, in addition to reduced angiogenesis, a similar shift toward increased $CD8^+$ T-cell function (18,19). Positive feedback control of COX-2 expression by COX-2-derived PGE_2 in tumors has been reported (57), raising the possibility that deletion of myeloid cell COX-2 disrupts tumor cell COX-2 expression, leading indirectly to the phenotype we observed in myeloid-COX-2 KO mice. We were unable to define by immunohistochemistry cell-specific COX-2 expression in WT and myeloid-COX-2 KO mammary tumor sections; however, the clear distinctions between our studies in epithelial or myeloid specific COX-2 KO models argues for independent functions of COX-2 in mammary epithelium and myeloid cells. Thus, in MEC–COX-2 KO mice, enhanced $CD8^+$ T-cell function was attributable to increased tumor expression of the T-cell chemokine CXCL9 and reduced tumor cell expression of the T-cell-suppressive programmed cell death-1 ligand 1 (PD-L1) (19). In contrast, neither PD-L1 (data not shown) nor T-cell chemoattractant molecules were modified in myeloid-COX-2 KO tumors, where instead reduced CSF-1R expression/macrophage infiltration and reduced TAM immunosuppressive function appear to be the dominant antitumorigenic effects. It appears therefore that, although both tumor cell and myeloid cell COX-2 can promote mammary tumorigenesis and regulate tumor immunity, there are distinct autocrine and paracrine functions of COX-2 in the two tumor components.

Given that CTL activity is typically attributed to induction of apoptosis through caspase-dependent mechanisms, it is, perhaps, surprising that caspase 3 expression in orthotopic and spontaneous myeloid-COX-2 KO tumors was unchanged compared with WT. It may be that, since detection of caspase 3 expression in whole tumors does not discriminate between cell populations, divergent changes in expression were occurring—for example in myeloid-COX-2 KO mice tumor cell caspase 3 may be elevated because of CTL-dependent apoptosis, whereas in WT mice, immunosuppressive macrophages may induce T-cell apoptosis (58,59). Alternatively, CTL-mediated perforin-granzyme A and granzyme B pathways can cause apoptosis through DNA damage without activating caspase pathways (60,61).

It is increasingly evident that a supportive tumor microenvironment is essential for tumor progression toward malignancy. Suppression of effector T-cell function can establish an area of immune privilege in which the tumor cells do not become exposed to tumoricidal T cells *in vivo* (62). In concordance, a stromal signature that is high in TAM and low in CTLs has been proposed as indicator of poor prognosis in human breast cancer (63). Indeed, depletion of macrophages through Csf^{op}/Csf^{op} mice, or treatment with liposome-encapsulated clondronate, led to a delayed histological progression to malignancy in a spontaneous mammary tumor model (13,64,65). Similarly, in other cancers, depletion of macrophages, or interference of CSF-1 signaling, led to reduced tumor growth, reduced metastasis and even induced tumor regression (66–68). We propose that targeted inhibition of COX-2 in myeloid cells may provide an approach to overcome immune privilege and enhance tumor immune surveillance. Macrophages are a tractable target for nanotherapeutic delivery (69,70) of COX-2 inhibitors or small interfering RNA that may allow for the antitumor benefit without the side effects of systemic COX-2 inhibition. Indeed, in contrast to global COX-2 KO or systemic pharmacological COX-2 inhibition, deletion of myeloid cell COX-2 in mice did not lead to increased thrombotic responses and actually reduced atherogenesis in hyperlipidemic mice (22), arguing for the CV safety of targeting macrophage COX-2 in cancer and other pathophysiologies.

Supplementary material

Supplementary Materials and methods and Supplementary Figures 1–5 can be found at http://carcin.oxfordjournals.org/

Funding

American Cancer Society grant (RSG0802401 to E.M.S); American Heart Association postdoctoral fellowship (AHA12POST11890008 to X.L.); National Institutes of Health grant (U54 HL11 7798 to T.G.); National Institutes of Health training grant (T32-GM08076 to E.P.C.).

Acknowledgements

The authors thank Dr Lewis Chodosh for the NAF and SMF cell lines. The authors also thank Mrs Ania W. Payne for assistance with orthotopic injections. Finally, the authors thank Ms Vicky N. Ndong, Mrs Jennifer Bruce and Dr Sarah Teegarden for technical assistance.

Conflicts of Interest Statement: None declared.

References

1. Smyth,E.M. *et al.* (2009) Prostanoids in health and disease. *J. Lipid Res.*, **50**, S423–S428.
2. Wang,D. *et al.* (2010) Eicosanoids and cancer. *Nat. Rev. Cancer*, **10**, 181–193.
3. Harris,R.E. (2009) Cyclooxygenase-2 (cox-2) blockade in the chemoprevention of cancers of the colon, breast, prostate, and lung. *Inflammopharmacology*, **17**, 55–67.
4. Howe,L.R. *et al.* (2005) HER2/neu-induced mammary tumorigenesis and angiogenesis are reduced in cyclooxygenase-2 knockout mice. *Cancer Res.*, **65**, 10113–10119.
5. Lanza-Jacoby,S. *et al.* (2003) The cyclooxygenase-2 inhibitor, celecoxib, prevents the development of mammary tumors in Her-2/neu mice. *Cancer Epidemiol. Biomarkers Prev.*, **12**, 1486–1491.
6. Keibel,A. *et al.* (2009) Inflammation, microenvironment, and the immune system in cancer progression. *Curr. Pharm. Des.*, **15**, 1949–1955.
7. Gordon,S. (2003) Alternative activation of macrophages. *Nat. Rev. Immunol.*, **3**, 23–35.
8. Sica,A. *et al.* (2006) Tumour-associated macrophages are a distinct M2 polarised population promoting tumour progression: potential targets of anti-cancer therapy. *Eur. J. Cancer*, **42**, 717–727.
9. Chang,C.I. *et al.* (2001) Macrophage arginase promotes tumor cell growth and suppresses nitric oxide-mediated tumor cytotoxicity. *Cancer Res.*, **61**, 1100–1106.
10. DeNardo,D.G. *et al.* (2011) Leukocyte complexity predicts breast cancer survival and functionally regulates response to chemotherapy. *Cancer Discov.*, **1**, 54–67.
11. Hernandez,L. *et al.* (2009) The EGF/CSF-1 paracrine invasion loop can be triggered by heregulin beta1 and CXCL12. *Cancer Res.*, **69**, 3221–3227.
12. Leek,R.D. *et al.* (1996) Association of macrophage infiltration with angiogenesis and prognosis in invasive breast carcinoma. *Cancer Res.*, **56**, 4625–4629.

13. Lin,E.Y. *et al.* (2006) Macrophages regulate the angiogenic switch in a mouse model of breast cancer. *Cancer Res*., **66**, 11238–11246.
14. Eruslanov,E. *et al.* (2010) Pivotal Advance: Tumor-mediated induction of myeloid-derived suppressor cells and M2-polarized macrophages by altering intracellular PGE2 catabolism in myeloid cells. *J. Leukoc. Biol*., **88**, 839–848.
15. Na,Y.R. *et al.* (2013) Cyclooxygenase-2 inhibition blocks M2 macrophage differentiation and suppresses metastasis in murine breast cancer model. *PLoS One*, **8**, e63451.
16. Chen,E.P. *et al.* (2011) COX-2 and PGE2-dependent immunomodulation in breast cancer. *Prostaglandins Other Lipid Mediat*., **96**, 14–20.
17. Greene,E.R. *et al.* (2011) Regulation of inflammation in cancer by eicosanoids. *Prostaglandins Other Lipid Mediat*., **96**, 27–36.
18. Markosyan,N. *et al.* (2011) Deletion of cyclooxygenase 2 in mouse mammary epithelial cells delays breast cancer onset through augmentation of type 1 immune responses in tumors. *Carcinogenesis*, **32**, 1441–1449.
19. Markosyan,N. *et al.* (2013) Mammary carcinoma cell derived cyclooxygenase 2 suppresses tumor immune surveillance by enhancing intratumoral immune checkpoint activity. *Breast Cancer Res*., **15**, R75.
20. Vardeh,D. et al. (2009) COX2 in CNS neural cells mediates mechanical inflammatory pain hypersensitivity in mice. *J Clin Invest,* **119**, 287–294.
21. Clausen,B.E. *et al.* (1999) Conditional gene targeting in macrophages and granulocytes using LysMcre mice. *Transgenic Res*., **8**, 265–277.
22. Hui,Y. *et al.* (2010) Targeted deletions of cyclooxygenase-2 and atherogenesis in mice. *Circulation*, **121**, 2654–2660.
23. Muller,W.J. *et al.* (1988) Single-step induction of mammary adenocarcinoma in transgenic mice bearing the activated c-neu oncogene. *Cell*, **54**, 105–115.
24. Elson,A. *et al.* (1995) Protein-tyrosine phosphatase epsilon. An isoform specifically expressed in mouse mammary tumors initiated by v-Ha-ras OR neu. *J. Biol. Chem*., **270**, 26116–26122.
25. Davies,J.Q. *et al.* (2005) Isolation and culture of murine macrophages. *Methods Mol. Biol*., **290**, 91–103.
26. Zhang,X. *et al.* (2008) The isolation and characterization of murine macrophages. *Curr. Protoc. Immunol*., **Chapter 14**, Unit 14.1.
27. Bookout,A.L. *et al.* (2003) Quantitative real-time PCR protocol for analysis of nuclear receptor signaling pathways. *Nucl. Recept. Signal*., **1**, e012.
28. Song,W.L. *et al.* (2007) Noninvasive assessment of the role of cyclooxygenases in cardiovascular health: a detailed HPLC/MS/MS method. *Methods Enzymol*., **433**, 51–72.
29. Ciccimaro,E. *et al.* (2010) Stable-isotope dilution LC–MS for quantitative biomarker analysis. *Bioanalysis*, **2**, 311–341.
30. Laoui,D. *et al.* (2011) Tumor-associated macrophages in breast cancer: distinct subsets, distinct functions. *Int. J. Dev. Biol*., **55**, 861–867.
31. Biswas,S.K. *et al.* (2006) A distinct and unique transcriptional program expressed by tumor-associated macrophages (defective NF-kappaB and enhanced IRF-3/STAT1 activation). *Blood*, **107**, 2112–2122.
32. DeNardo,D.G. *et al.* (2009) CD4(+) T cells regulate pulmonary metastasis of mammary carcinomas by enhancing protumor properties of macrophages. *Cancer Cell*, **16**, 91–102.
33. Van Ginderachter,J.A. *et al.* (2006) Classical and alternative activation of mononuclear phagocytes: picking the best of both worlds for tumor promotion. *Immunobiology*, **211**, 487–501.
34. Xu,J. *et al.* (2013) CSF1R signaling blockade stanches tumor-infiltrating myeloid cells and improves the efficacy of radiotherapy in prostate cancer. *Cancer Res*., **73**, 2782–2794.
35. Aerts,J.G. *et al.* (2013) Tumor-specific cytotoxic T cells are crucial for efficacy of immunomodulatory antibodies in patients with lung cancer. *Cancer Res*., **73**, 2381–2388.
36. Mocellin,S. *et al.* (2013) CTLA-4 blockade and the renaissance of cancer immunotherapy. *Biochim. Biophys. Acta*, **1836**, 187–196.
37. Coussens,L.M. *et al.* (2013) Neutralizing tumor-promoting chronic inflammation: a magic bullet? *Science*, **339**, 286–291.
38. Topalian,S.L. *et al.* (2012) Safety, activity, and immune correlates of anti-PD-1 antibody in cancer. *N. Engl. J. Med*., **366**, 2443–2454.
39. Grosser,T. *et al.* (2006) Biological basis for the cardiovascular consequences of COX-2 inhibition: therapeutic challenges and opportunities. *J. Clin. Invest*., **116**, 4–15.
40. Saccani,A. *et al.* (2006) p50 nuclear factor-kappaB overexpression in tumor-associated macrophages inhibits M1 inflammatory responses and antitumor resistance. *Cancer Res*., **66**, 11432–11440.
41. Friend,S.H. *et al.* (1986) A human DNA segment with properties of the gene that predisposes to retinoblastoma and osteosarcoma. *Nature*, **323**, 643–646.
42. Mantovani,A. *et al.* (2002) Macrophage polarization: tumor-associated macrophages as a paradigm for polarized M2 mononuclear phagocytes. *Trends Immunol*., **23**, 549–555.
43. Nakanishi,Y. *et al.* (2011) COX-2 inhibition alters the phenotype of tumor-associated macrophages from M2 to M1 in ApcMin/+ mouse polyps. *Carcinogenesis*, **32**, 1333–1339.
44. Crofford,L.J. *et al.* (1997) Involvement of nuclear factor kappa B in the regulation of cyclooxygenase-2 expression by interleukin-1 in rheumatoid synoviocytes. *Arthritis Rheum*., **40**, 226–236.
45. Ulivi,V. *et al.* (2008) p38/NF-kB-dependent expression of COX-2 during differentiation and inflammatory response of chondrocytes. *J. Cell. Biochem*., **104**, 1393–1406.
46. Hagemann,T. *et al.* (2008) "Re-educating" tumor-associated macrophages by targeting NF-kappaB. *J. Exp. Med*., **205**, 1261–1268.
47. Lacey,D.C. *et al.* (2012) Defining GM-CSF- and macrophage-CSF-dependent macrophage responses by *in vitro* models. *J. Immunol*., **188**, 5752–5765.
48. Pollard,J.W. (2004) Tumour-educated macrophages promote tumour progression and metastasis. *Nat. Rev. Cancer*, **4**, 71–78.
49. Kusmartsev,S. *et al.* (2005) STAT1 signaling regulates tumor-associated macrophage-mediated T cell deletion. *J. Immunol*., **174**, 4880–4891.
50. Fridlender,Z.G. *et al.* (2009) Polarization of tumor-associated neutrophil phenotype by TGF-beta: "N1" versus "N2" TAN. *Cancer Cell*, **16**, 183–194.
51. Sinha,P. *et al.* (2007) Prostaglandin E2 promotes tumor progression by inducing myeloid-derived suppressor cells. *Cancer Res*., **67**, 4507–4513.
52. Lukkarinen,H. *et al.* (2006) Inhibition of COX-2 aggravates neutrophil migration and pneumocyte apoptosis in surfactant-depleted rat lungs. *Pediatr. Res*., **59**, 412–417.
53. Liao,C.J. *et al.* (2012) The cancer marker neutrophil gelatinase-associated lipocalin is highly expressed in human endometrial hyperplasia. *Mol. Biol. Rep*., **39**, 1029–1036.
54. Buchanan,F.G. *et al.* (2003) Prostaglandin E2 regulates cell migration via the intracellular activation of the epidermal growth factor receptor. *J. Biol. Chem*., **278**, 35451–35457.
55. Pai,R. *et al.* (2002) Prostaglandin E2 transactivates EGF receptor: a novel mechanism for promoting colon cancer growth and gastrointestinal hypertrophy. *Nat. Med*., **8**, 289–293.
56. Sheng,H. *et al.* (1998) Modulation of apoptosis and Bcl-2 expression by prostaglandin E2 in human colon cancer cells. *Cancer Res*., **58**, 362–366.
57. Obermajer,N. *et al.* (2011) Positive feedback between PGE2 and COX2 redirects the differentiation of human dendritic cells toward stable myeloid-derived suppressor cells. *Blood*, **118**, 5498–5505.
58. Badley,A.D. *et al.* (1997) Macrophage-dependent apoptosis of CD4+ T lymphocytes from HIV-infected individuals is mediated by FasL and tumor necrosis factor. *J. Exp. Med*., **185**, 55–64.
59. Saio,M. *et al.* (2001) Tumor-infiltrating macrophages induce apoptosis in activated CD8(+) T cells by a mechanism requiring cell contact and mediated by both the cell-associated form of TNF and nitric oxide. *J. Immunol*., **167**, 5583–5593.
60. Trapani,J.A. *et al.* (1998) Efficient nuclear targeting of granzyme B and the nuclear consequences of apoptosis induced by granzyme B and perforin are caspase-dependent, but cell death is caspase-independent. *J. Biol. Chem*., **273**, 27934–27938.
61. Trapani,J.A. *et al.* (2002) Functional significance of the perforin/granzyme cell death pathway. *Nat. Rev. Immunol*., **2**, 735–747.
62. Vonderheide,R.H. *et al.* (2013) Inflammatory networks and immune surveillance of pancreatic carcinoma. *Curr. Opin. Immunol*., **25**, 200–205.
63. Finak,G. *et al.* (2008) Stromal gene expression predicts clinical outcome in breast cancer. *Nat. Med*., **14**, 518–527.
64. Lin,E.Y. *et al.* (2001) Colony-stimulating factor 1 promotes progression of mammary tumors to malignancy. *J. Exp. Med*., **193**, 727–740.
65. Qian,B. *et al.* (2009) A distinct macrophage population mediates metastatic breast cancer cell extravasation, establishment and growth. *PLoS One*, **4**, e6562.
66. Kacinski,B.M. (1997) CSF-1 and its receptor in breast carcinomas and neoplasms of the female reproductive tract. *Mol. Reprod. Dev*., **46**, 71–74.
67. Beck,A.H. *et al.* (2009) The macrophage colony-stimulating factor 1 response signature in breast carcinoma. *Clin. Cancer Res*., **15**, 778–787.
68. Partecke,L.I. *et al.* (2013) Induction of M2-macrophages by tumour cells and tumour growth promotion by M2-macrophages: a quid pro quo in pancreatic cancer. *Pancreatology*, **13**, 508–516.
69. Leuschner,F. *et al.* (2011) Therapeutic siRNA silencing in inflammatory monocytes in mice. *Nat. Biotechnol*., **29**, 1005–1010.
70. Gu,X. *et al.* (2011) Preparation and characterization of a lovastatin-loaded protein-free nanostructured lipid carrier resembling high-density lipoprotein and evaluation of its targeting to foam cells. *AAPS PharmSciTech*, **12**, 1200–1208.

Received October 17, 2013; revised February 3, 2014;
accepted February 22, 2014